

Tunable single mode lasing from an on-chip optofluidic ring resonator laser

Wonsuk Lee, Hao Li, Jonathan D. Suter, Karthik Reddy, Yuze Sun et al.

Citation: *Appl. Phys. Lett.* **98**, 061103 (2011); doi: 10.1063/1.3554362

View online: <http://dx.doi.org/10.1063/1.3554362>

View Table of Contents: <http://apl.aip.org/resource/1/APPLAB/v98/i6>

Published by the AIP Publishing LLC.

Additional information on *Appl. Phys. Lett.*

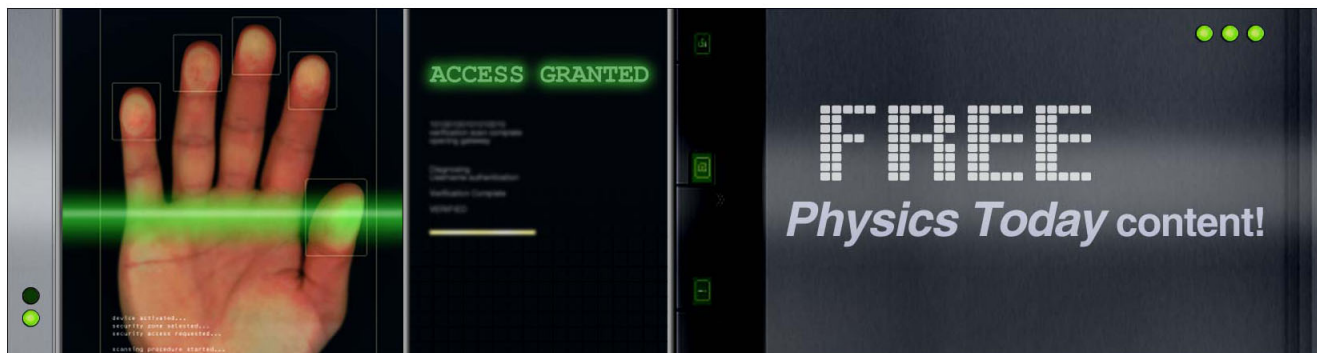
Journal Homepage: <http://apl.aip.org/>

Journal Information: http://apl.aip.org/about/about_the_journal

Top downloads: http://apl.aip.org/features/most_downloaded

Information for Authors: <http://apl.aip.org/authors>

ADVERTISEMENT



Tunable single mode lasing from an on-chip optofluidic ring resonator laser

Wonsuk Lee,^{1,2} Hao Li,^{1,3} Jonathan D. Suter,¹ Karthik Reddy,^{1,2} Yuze Sun,¹ and Xudong Fan^{1,a)}

¹Department of Biomedical Engineering, University of Michigan, 1101 Beal Ave., Ann Arbor, Michigan 48109, USA

²Department of Electrical Engineering and Computer Science, University of Michigan, Ann Arbor, Michigan 48109, USA

³Department of Optical Science and Engineering, Key Laboratory for Micro and Nano Photonic Structures (Ministry of Education), Fudan University, Shanghai 200433, People's Republic of China

(Received 14 November 2010; accepted 21 January 2011; published online 8 February 2011)

Single mode lasing from the polydimethylsiloxane based on-chip coupled optofluidic ring resonator (OFRR) with the lasing threshold of a few $\mu\text{J}/\text{mm}^2$ is demonstrated using the Vernier effect. The single mode operation is highly stable even at high pump energy densities. The effect of the OFRR size and coupling strength on the single mode emission is investigated, showing that the excessive coupling results in incomplete side mode suppression. Tuning of the lasing wavelength is achieved by modifying the dye solution. © 2011 American Institute of Physics. [doi:10.1063/1.3554362]

Optofluidic dye lasers have been intensively investigated because of their potential of integration in lab-on-a-chip devices and wavelength tunability.^{1,2} As compared to other types of optical cavities explored for optofluidic lasers, such as Fabry–Perot resonators^{3–5} and distributed-feedback (DFB) gratings,^{6–8} optofluidic ring resonators (OFRRs) that support the circulating resonant waveguide mode or the whispering gallery mode take advantage of compact size and relatively high Q-factors, both of which are a key to achieving large scale integration and low lasing thresholds. The OFRR lasers have previously been implemented in the form of discrete ring cavities,⁹ microdroplets,¹⁰ microknots,¹¹ microcylinders,^{12–14} and microcapillaries.^{15,16} Very recently, on-chip polydimethylsiloxane (PDMS) based OFRRs were also demonstrated.^{17,18} Since the entire PDMS device can be fabricated by simple replica molding processes, cost-effective mass production of the OFRR lasers becomes possible.

However, the OFRR laser intrinsically has multimode lasing emission due to its narrow free spectral range (FSR), which is a major drawback as compared to the DFB based optofluidic laser capable of single mode operation. One of the methods to suppress side modes is to utilize the Vernier effect, in which two ring resonators of different FSRs are coupled to each other. While the single mode laser emission has been achieved in on-chip solid coupled ring resonators,¹⁹ on-chip OFRR single mode lasers and their lasing characteristics have not been studied.

In this letter, we develop and characterize the single mode laser using a PDMS based coupled OFRR. The effect of the OFRR size and coupling strength on the single mode emission is investigated, and the tuning of the lasing wavelength is demonstrated. We show that stable single mode laser emission can be obtained with the lasing threshold on the order of a few $\mu\text{J}/\text{mm}^2$.

Figure 1(a) shows a schematic of the coupled OFRR laser system consisting of two size mismatched ring resonators

and a liquid-filled waveguide. It is produced in PDMS by a replica molding process. The master mold is first fabricated on a silicon wafer by photolithography and reactive ion etching. The wafer is then vacuum-coated with trichlorosilane and subsequently coated with uncured PDMS. Finally, the PDMS is cured at room temperature for 48 h before it is peeled off from the wafer and treated with O_2 plasma. The resulting circular and straight liquid channels are shown in Figs. 1(b) and 1(c), which are $40\ \mu\text{m}$ in width and $10\ \mu\text{m}$ in depth. The two ring resonators (the lower ring and the straight waveguide) are optically coupled but physically disconnected. During the experiment, dye dissolved in tetraethylene glycol (TEG) is introduced into the two OFRRs, whereas the waveguide is filled with TEG alone. Since the refractive index (RI) of TEG (1.456) is larger than that of PDMS (1.42), light is confined in the gain medium and the liquid waveguide. The coupled OFRR is uniformly pumped

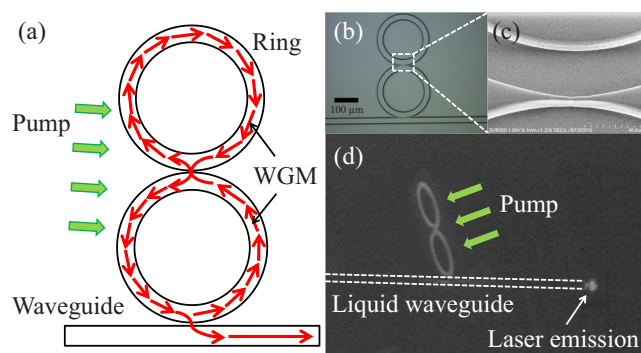


FIG. 1. (Color online) (a) Schematic of a coupled OFRR laser. The arrows inside the ring resonator show light propagation direction. (b) Image of the coupled OFRR formed on the PDMS substrate. The diameter of the upper (lower) ring is $290\ (300)\ \mu\text{m}$. The gaps between the lower ring and the waveguide and between the two rings are $2\ \text{and}\ 1\ \mu\text{m}$, respectively. The two rings are filled with dye dissolved in TEG, whereas the waveguide is filled with TEG alone. (c) Scanning electron microscopic image of the $1\ \mu\text{m}$ gap between the two rings. (d) Photograph of the coupled OFRR during laser operation. The laser emission is coupled into the liquid waveguide and collected at its distal end. Dashed lines show the waveguide position.

^{a)}Electronic mail: xsfan@umich.edu.

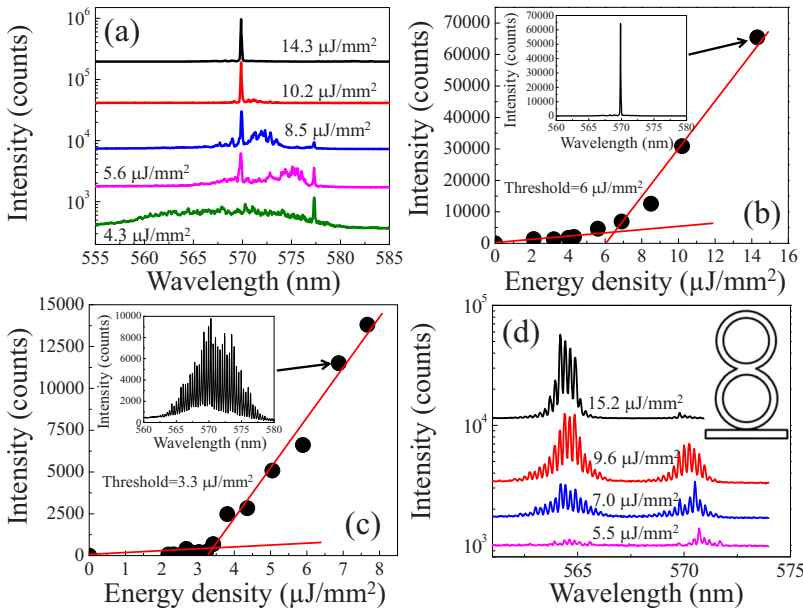


FIG. 2. (Color online) (a) Lasing spectra of the coupled OFRR laser described in Fig. 1(b) at various pump energy densities. Curves are vertically shifted for clarity. (b) Intensity of the laser emission at 569.9 nm as a function of the pump energy density. Inset: lasing spectrum when the pump energy density is 14.3 $\mu\text{J}/\text{mm}^2$. (c) Intensity of the laser emission from a single OFRR of 300 μm in diameter. Inset: lasing spectrum when the pump energy density is 6.9 $\mu\text{J}/\text{mm}^2$. (d) Lasing spectra of the coupled OFRR laser when the two rings are in contact (contact region = 19 μm). Curves are vertically shifted for clarity. 2 mM R6G is used in the experiments.

by a 5 ns pulsed optical parametric oscillator at 532 nm, as illustrated in Figs. 1(a) and 1(d). The lasing emission is coupled into the liquid waveguide near the lower OFRR and detected at its distal end by a spectrometer (Horiba iHR550, resolution of 0.06 nm).

The lasing spectra of the coupled OFRR filled with 2 mM R6G at various pump energy densities are plotted in Fig. 2(a). At the lowest pump energy density, the single mode lasing emission occurs at 577.3 nm, whose lasing threshold is about 3 $\mu\text{J}/\text{mm}^2$. As the pump energy density increases, another strong mode emerges at 569.9 nm. These two modes result from the Vernier effect. In fact, the 7.4 nm spectral separation agrees well with the FSR calculated based on the Vernier equation $\Delta\lambda = \lambda^2 / \pi n_{\text{eff}} (D_1 - D_2)$, where λ (=575 nm), n_{eff} (=1.456), D_1 (=300 μm), and D_2 (=290 μm) are the lasing wavelength, the effective RI of the ring resonator, and the ring diameters, respectively. When the pump energy density continues to increase, the lasing at the Vernier mode at 577.3 nm diminishes, whereas the strong and robust single mode lasing is sustained at another Vernier mode at 569.9 nm. This blueshift of the mode is attributed to the gain profile change under high pump intensities, as described earlier.²⁰ The linewidth of this 569.9 nm mode is approximately 0.06 nm, limited by the spectrometer resolution. The corresponding lasing threshold curve is plotted in Fig. 2(b) with the lasing threshold of about 6 $\mu\text{J}/\text{mm}^2$. For comparison, the spectrum from a single OFRR laser (lower ring alone) is depicted in the inset of Fig. 2(c), showing the

typical multimode lasing emission, which further confirms the Vernier effect on the single mode lasing operation. The lasing threshold in Fig. 2(c) is approximately 3.3 $\mu\text{J}/\text{mm}^2$.

Coupling between the two OFRRs plays an important role in obtaining the single mode lasing through the Vernier effect. Whereas inefficient coupling results in insufficient optical feedback provided by one ring to another, excessive coupling broadens the resonance linewidth (or decreases the Q-factor) of each OFRR. Both lead to degradation in side mode suppression. The coupling coefficient between the two OFRRs, κ , can be calculated by the coupled mode theory.^{21,22} Figure 3 presents the coupling coefficients among the first three orders of the modes in the coupled OFRR in Fig. 1(b). The coupling related Q-factor, given by $n_{\text{eff}} \pi^2 D / \lambda \kappa^2$, should exceed 10^8 . Similarly, we calculate the total coupling coefficient between the lower OFRR and the waveguide (i.e., total fractional loss per round trip of the lower OFRR) to be on the order of 10^{-3} , corresponding to a $Q \sim 7 \times 10^6$. Therefore, based on the Q-factor (~ 5000) experimentally observed in a single PDMS based OFRR in our previous studies,¹⁸ we infer that each ring in the current coupled OFRR system should have a similar Q-factor (~ 5000), which provides sufficient side mode suppression to achieve single mode operation, as shown in Fig. 2(a).

In contrast, in Fig. 2(d), the two rings are in contact with the width of the connected region of about 19 μm . In this case, the Q-factor of the OFRR is significantly spoiled due to

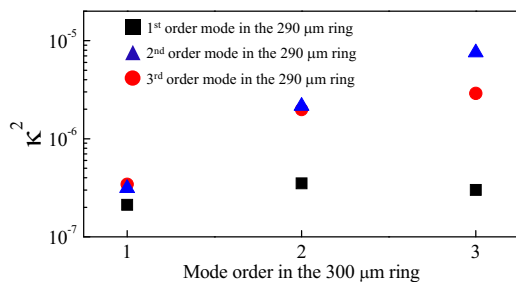


FIG. 3. (Color online) Coupling coefficient between the modes of the OFRRs described in Fig. 1(b).

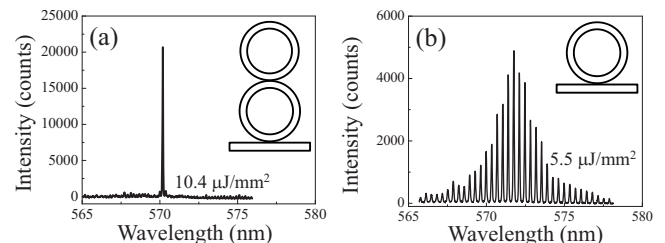


FIG. 4. (a) Lasing spectrum from a coupled OFRR (190 and 200 μm in diameter, respectively). The gaps between the lower ring and the waveguide and between the two rings are 2 and 1 μm , respectively. (b) Lasing spectrum from a single OFRR (200 μm in diameter). Gain medium is 2 mM R6G in TEG.

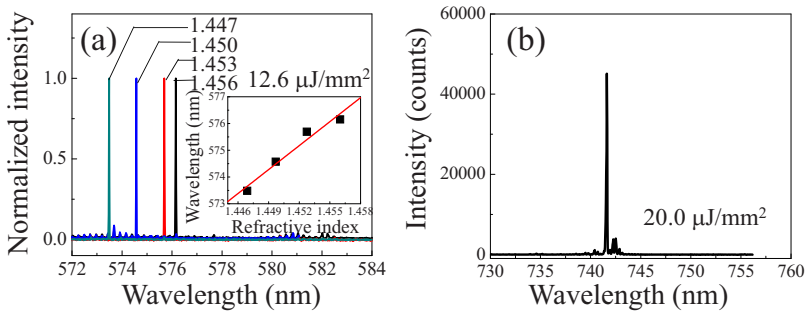


FIG. 5. (Color online) (a) Lasing spectra of the coupled OFRR laser described in Fig. 1(b) when the RI of 2 mM R6G solvent is varied by adding methanol to TEG. Inset: lasing wavelength as a function of solvent RI. (b) Lasing spectrum from 2 mM LDS 722 in TEG.

the excessive coupling loss between the two rings. As a result, although the Vernier effect is still present (as evidenced by the clustered peaks separated by about 6 nm), it fails to completely suppress side modes, leading to the emergence of well-spaced lasing modes modulated by the Vernier modes. The distance of the two adjacent modes is 0.235 nm, corresponding to the FSR of the 300 μm diameter OFRR. Although the coupled mode theory becomes invalid for us to calculate the coupling related Q-factor, it is estimated to be approximately 500 based on the Vernier mode profile in Fig. 2(d). This Q-factor value is close to what was observed previously, in which the ring resonator has a similar contact region with a waveguide.¹⁸

While the coupling between the two OFRRs affects the single mode operation of the OFRR laser, the size of the OFRRs does not deteriorate the properties of the lasing. As illustrated in Fig. 4(a), the single mode lasing can be achieved in the coupled OFRRs with the respective diameters of 190 and 200 μm . According to the coupled mode theory, the coupling related loss is still negligible. As a result, the Q-factor of the OFRR (still a few thousands) is sufficient to suppress the side modes. Once again, in order to verify the Vernier effect, Fig. 4(b) shows the multimode lasing from the lower OFRR alone in the absence of the upper OFRR.

Since the lasing wavelength of the coupled OFRR laser is determined by the common resonant mode in the two OFRRs, the lasing wavelength can be tuned by changing the RI of the gain medium according to $\Delta\lambda/\lambda = \Delta n_{\text{eff}}/n_{\text{eff}}$, where $\Delta\lambda$ and Δn_{eff} are the resonance wavelength change and the effective RI change, respectively. Since Δn_{eff} and n_{eff} are nearly the same for both OFRRs, the common mode in both OFRRs can be tuned synchronously to ensure the single mode lasing over a broad spectral range. Figure 5(a) shows such wavelength tuning by dissolving 2 mM R6G into the mixture of TEG and methanol (RI=1.36) whose RI is varied by the proportion of methanol and TEG. As depicted in the inset of Fig. 5(a), the lasing wavelength clearly shows a linear relationship with the RI. To tune the lasing wavelength over an even large spectral range, a different dye solution is injected to the same coupled OFRR structure. Figure 4(b) shows the single mode lasing at 741.6 nm from the coupled OFRR using 2 mM LDS 722 in TEG.

In summary, we have demonstrated the single mode lasing from the coupled OFRR via the Vernier effect. The single mode operation is stable even under high pump energy densities. It is not affected by the size of the laser cavity or the gain medium used, thus allowing us to use different sizes of

the OFRRs for optimal lasing performance and to tune the lasing wavelength over various spectral ranges. Our study further shows that coupling between the OFRRs plays an important role in achieving the single mode lasing. Excessive coupling may spoil the Q-factor and result in incomplete side mode suppression. The tunable single mode lasing, low lasing threshold, cost-effective mass production, and the capability of coupling the lasing emission into a liquid channel make the PDMS based OFRR system a highly competitive technology in the development of optofluidic lasers and lab-on-a-chip devices.

This work was supported by the NSF (Grant Nos. ECCS-1045621 and CBET-1037097).

- ¹C. Monat, P. Domachuk, and B. J. Eggleton, *Nat. Photonics* **1**, 106 (2007).
- ²A. R. Hawkins and H. Schmidt, *Handbook of Optofluidics* (CRC, Boca Raton, FL, 2010).
- ³B. Helbo, A. Kristensen, and A. Menon, *J. Micromech. Microeng.* **13**, 307 (2003).
- ⁴D. V. Vezenov, B. T. Mayers, R. S. Conroy, G. M. Whitesides, P. T. Snee, Y. Chan, D. G. Nocera, and M. G. Bawendi, *J. Am. Chem. Soc.* **127**, 8952 (2005).
- ⁵Q. Kou, I. Yesilyurt, and Y. Chen, *Appl. Phys. Lett.* **88**, 091101 (2006).
- ⁶Z. Y. Li, Z. Y. Zhang, T. Emery, A. Scherer, and D. Psaltis, *Opt. Express* **14**, 696 (2006).
- ⁷W. Song, A. E. Vasdekis, Z. Li, and D. Psaltis, *Appl. Phys. Lett.* **94**, 161110 (2009).
- ⁸C. Vannahme, M. B. Christiansen, T. Mappes, and A. Kristensen, *Opt. Express* **18**, 9280 (2010).
- ⁹J. C. Galas, J. Torres, M. Belotti, Q. Kou, and Y. Chen, *Appl. Phys. Lett.* **86**, 264101 (2005).
- ¹⁰H.-M. Tzeng, K. F. Wall, M. B. Long, and R. K. Chang, *Opt. Lett.* **9**, 499 (1984).
- ¹¹X. Jiang, Q. Song, L. Xu, J. Fu, and L. Tong, *Appl. Phys. Lett.* **90**, 233501 (2007).
- ¹²J. C. Knight, H. S. T. Driver, R. J. Hutcheon, and G. N. Robertson, *Opt. Lett.* **17**, 1280 (1992).
- ¹³H.-J. Moon, Y.-T. Chough, and K. An, *Phys. Rev. Lett.* **85**, 3161 (2000).
- ¹⁴Y. Sun, J. D. Suter, and X. Fan, *Opt. Lett.* **34**, 1042 (2009).
- ¹⁵S. I. Shopova, H. Zhu, and X. Fan, *Appl. Phys. Lett.* **90**, 221101 (2007).
- ¹⁶Y. Sun, S. I. Shopova, C.-S. Wu, S. Arnold, and X. Fan, *Proc. Natl. Acad. Sci. U.S.A.* **107**, 16039 (2010).
- ¹⁷Z. Li, Z. Zhang, A. Scherer, and D. Psaltis, *IEEE/LEOS Summer Topical Meeting* (IEEE, Portland, OR, 2007), pp. 70–71.
- ¹⁸J. D. Suter, W. Lee, D. J. Howard, E. Hoppmann, I. M. White, and X. Fan, *Opt. Lett.* **35**, 2997 (2010).
- ¹⁹L. Shang, L. Liu, and L. Xu, *Opt. Lett.* **33**, 1150 (2008).
- ²⁰H.-J. Moon, Y.-T. Chough, J. B. Kim, K. An, J. Yi, and J. Lee, *Appl. Phys. Lett.* **76**, 3679 (2000).
- ²¹B. E. Little, J.-P. Laine, and H. A. Haus, *J. Lightwave Technol.* **17**, 704 (1999).
- ²²I. M. White, H. Oveys, X. Fan, T. L. Smith, and J. Zhang, *Appl. Phys. Lett.* **89**, 191106 (2006).